A Computational Study of the Hydration of the OH Radical

S. Hamad, S. Lago, and J. A. Mejías*

Departamento de Ciencias Ambientales, Universidad Pablo de Olavide, Carretera de Utrera, Km 1, 41013 Sevilla, Spain

Received: September 13, 2001; In Final Form: April 19, 2002

The OH radical is an important species in natural and man made aqueous environments, influencing diverse processes such as the oxidation of atmospheric pollutants or the development of some diseases. Yet, little is known about the solvation thermodynamics and structure of the hydration shell of OH. Here, we present a computational study of the hydration of OH in small $H_{2n+1}O_{n+1}$ ($n = 1-5$) clusters. We begin by comparing three different quantum chemical methods, UMP2, BLYP, and BHLYP. We find that BLYP does not describe correctly the OH−H_2O interaction as compared to the current MP2 or other high ab initio calculations found in the literature. BLYP favors the formation of hemibonded H_2O−OH structures, whereas MP2 predicts that hydrogen-bonded complexes are more stable. Mixing Becke's exchange functional with 50% Hartree−Fock exchange improves the DFT description, yielding results that are similar to those from MP2. We find that the $H_{2n+1}O_{n+1}$ clusters form structures in which all species are donors and acceptors in hydrogen bonded rings similar to those of pure water clusters. OH participates in two or three hydrogen bonds. Structures in which OH forms more than three hydrogen bonds are not favored energetically. We report values of energy, enthalpy, and Gibbs free energy of complexation in the gas phase, $OH(g) + H_{2n}O_n(g) \rightarrow H_{2n+1}O_{n+1}(g)$, as a function of cluster size. We also estimate values of thermodynamic parameters of hydration in the liquid phase from $OH(g) + H_{2n}O_n(aq) \rightarrow H_{2n+1}O_{n+1}(aq)$, where the energies of the aqueous species, $H_{2n}O_n(aq)$ and $H_{2n+1}O_{n+1}$-(aq), are calculated by means of a hybrid solvation model in which part of the solvent is treated explicitly and the long-range interactions are added into the Hamiltonian by means of the PCM version of the self-consistent reaction field. The implications of our work as well as the accuracy of the results are also discussed.

I. Introduction

The hydroxyl radical is thermodynamically and kinetically a powerful oxidant in aqueous environments.[1,2] It is formed by various mechanisms including the reaction of Fe(II) with H_2O_2 and the photolysis of dissolved species such as NO_3^-, NO_2^-, and O_3. It is also formed by radiolysis of liquid water,[3,4] with important applications such as radiotherapy or the removal of heavy metals from contaminated waters.[5,6] Other advanced oxidation processes for elimination of pollutants in water are based on the production of dissolved OH by heteregeneous photocatalysts.[7,8] OH radicals in natural waters react principally with dissolved organic matter, participating in the abstraction of H atoms or addition to C−C double bonds.[1] Tropospheric OH is dissolved in cloud droplets or formed in solution by decomposition of HO_2 and further reaction with ozone.[9,10] OH oxidizes soluble tropospheric organic molecules.[11] Recently, it has been found that OH radicals produced chemically are able to induce apoptosis in human tumor cells, which has been linked to a direct chemical effect of aqueous OH on telomere shortening.[12] Chemical reactions of OH in abnormally high concentrations in the cell cytoplasm have also been suggested to be responsible of Parkinson's disease.[13] The oxidation mechanism of organic molecules by aqueous OH is an active field of research.[14,15] Thus, a study of the hydration structure and thermodynamics of OH is important for the understanding of its rich chemistry in aqueous natural and man made environments. Additionally, the calculation of the hydration energy of OH is required for the assessment of the band gap of water owing to the large solvent reorganization energy in the photoemission process in this liquid.[16] Values of the thermodynamic parameters of OH hydration are also needed in the modeling of the uptake of OH radicals in aqueous surfaces.[17,18] For example, the uptake coefficient, γ, defined as the ration between the net number of molecules dissolving in the liquid phase and the number of molecules colliding with the liquid, can be calculated as

$$\frac{1}{\gamma} = \frac{1}{\alpha} + \frac{\upsilon_m}{4HRTDE}$$

where α is the accommodation coefficient (a rate parameter corresponding to the mass transfer at the interface), υ_m is the molecular velocity above the surface, R is the gas constant, T is absolute temperature, and E is the concentration gradient just below the surface. H is the Henry's law constant, $H = \exp(-\Delta G_{hyd}/RT)$, and ΔG_{hyd} is the hydration free energy of OH. The $H_{2n+1}O_{n+1}$ clusters are representative of the gas-phase hydration of the radical in the atmosphere, where OH plays a key role and small water aggregates have been proposed as catalysts in atmospheric reactions.[19,20] From the standpoint of a more basic research, the comparison between the hydration energies calculated from models and those measured in experiments provides information on the mechanism whereby the OH radical hydrates as well as the performance of the different theoretical methods for this sort of systems.

Despite the relevance of the interaction of OH with an aqueous environment, previous works on the hydrogen bonding

* To whom correspondence should be addressed: Phone: 00-3495-4349315. Fax: 00-3495-4349204. E-mail: jamejrom@dex.upo.es.

10.1021/jp013531y CCC: $22.00
Published on Web 09/11/2002

ability, the structure of the hydration shell, and the solvation thermodynamics of this molecule are scarce. The hydration free energy of OH was assessed from the oxidation potential of the radical, as measured from the equilibrium between OH and thallium(II) (ref 21). The reported standard free energy of hydration at room temperature was $\Delta G^0_{hyd}(OH) = -10.0$ kJ/mol. That value was interpreted in terms of the hydrogen bonding ability of this molecule with water and by assuming that a OH radical has three hydrogen bonding sites, one on the proton and two on the oxygen. A more recent calculation of the hydration energy of OH was reported in the context of the determination of the band gap of water.[16] The hydration energy was estimated by means of $H_{2n-1}O_n$ ($n = 1-15$) clusters and semiempirical PM3 calculations. The extrapolated hydration energy is $\Delta E_{hyd}(OH) = -35.70$ kJ/mol. This last quantity is a potential energy change, as calculated directly from geometry optimizations. Unfortunately, no structural information on the microsolvation environment was reported in that work.

The interaction of OH with a single water molecule has been studied recently by means of ab initio methods.[22] It was found that the most stable structure of the $OH-H_2O$ complex consists of OH acting as a donor in a hydrogen bond to water. This interaction is found to be slightly stronger, by 1−2 kJ/mol, than the hydrogen bond in the water dimer. The $HO-H_2O$ complex, in which the water molecule acts as a hydrogen donor, is less stable than the $H_2O\cdots HO$ configuration by about 10 kJ/mol. The interaction of OH with several water molecules was investigated in the context of small charged water clusters that contain OH along with H_3O^+ species.[23] In that work, it was found that structures in which the OH acts as proton acceptor are more stable (by 20−70 kJ/mol) than those in which the OH is both proton donor and acceptor. A preferential ordering of the cluster around the H_3O^+ ion may cause this. The oxygen in a water molecule bears a charge that is more negative than the charge on the oxygen of OH. Thus, H_3O^+ is preferentially solvated by water rather than by the radical. In its turn, the solvating waters act most favorably as proton donors in the hydrogen bonds to OH owing to the polarizing effect of the proton.

Other recent ab initio studies of OH radicals have tackled the adsorption onto oxide surfaces,[24] the reactions of polycyclic aromatic hydrocarbons with OH,[25] the hydrogen bonding to hydrogen peroxide,[26] the addition of the radical to dimethyl sulfide,[27] and the production of OH radicals by carbonyl oxides in solution phase.[28] In this last work, the solvent (acetonitrile) effects were considered in a simplified manner by means of a polarizable continuum. These solvent effects were shown to be important for the stabilization of reaction intermediates, lowering the barrier for the formation of OH.

The aims of the present work are 3-fold. First, we address the microsolvation of OH in small $H_{2n+1}O_{n+1}$ ($n = 1-5$) clusters by means of three different quantum chemical methods. We begin our study by using density functional theory (DFT)[29] with the Becke exchange potential[30] and the Lee−Yang−Parr (LYP) correlation potential[31] (BLYP). One of the advantages of this functional is that it does not contain Hartree−Fock exchange, which simplifies the computational procedures, speeding up the calculations. However, it has been shown repeatedly that the lack of exact exchange leads to an overestimation of the self-interaction part of the exchange energy for the three electron bonds,[32,33] which in this cause might arise from the interaction between the unpaired electron in OH and the lone pairs of H_2O. For example, it has been shown that the ground state of the $H_4O_2^+$ cation is wrongly predicted by pure DFT methods (LDA, BLYP, and BP86) to be a hemibonded structure with a three electron bond between two H_2O fragments.[34] Accurate MP2 and CCSD(T) calculations predict that the $OH-H_2O^+$ structure is the true ground state. It has also been shown that DFT can provide the correct description of the $H_4O_2^+$ system by using a hybrid functional that mixes some exact exchange within the exchange functional. This prompted us to do UHF-MP2 calculations along with DFT with the Becke's half and half (BH) functional[35] combined with the LYP correlation (BHLYP). The comparison between BLYP and MP2 calculations shows that the BLYP description incorrectly favors a hemibonded-like structure for the $H_{2n+1}O_{n+1}$ complexes for $n = 1-3$. For $n = 4-5$, the structures predicted by BLYP are more similar to those found by MP2. Our results also show that the BHLYP method yields results that are similar to those from MP2 calculations, although some differences in the energies and structures remain.

Our second aim is to report thermodynamic data for the interaction between OH and small water clusters in the gas phase, $OH(g) + H_{2n}O_n(g) \rightarrow H_{2n+1}O_{n+1}(g)$ that is of interest for the description of atmospheric reactions in which the OH radical participates. The thermodynamics for the gas phase is worked out from the energies of the optimized $H_{2n+1}O_{n+1}$ clusters as well as the computed harmonic vibrational frequencies. This allows the enthalpies and free energies to be calculated. We also make use of the ideal gas traslational and rotational energies and partition functions for the enthalpy and entropy contributions.

A third goal is to obtain data on the solvation thermodynamics of OH in liquid water at room temperature. This is achieved by using a hybrid model of solvation. The first solvation shell of OH is modeled by the gas-phase $H_{2n+1}O_{n+1}$ cluster and the long range solvent effects are taken into account by means of a self-consistent reaction field method.[36] This combination of explicit and continuum solvent models is not new and has been extensively used for ionic solvation.[37−43] For many ions in water, the strong electrostatic interactions with the solute lead to well defined structures for the hydration shell, especially in the case of highly charged cations and the proton. In these cases, the most likely structure of the hydration shell is well defined, with other structures being much higher in energy. Thus, the explicit part of the solvent is well modeled by a single structure. For ions that interact less strongly with the solvent, it has been suggested that several candidate geometries of the explicit hydration shell must be investigated.[41] In this case, the thermodynamic parameters are constructed by performing a Boltzmann weighting over the different geometries. We have followed this procedure for $H_{2n+1}O_{n+1}$ clusters with $n = 4$ and 5. Another issue that has to be tackled is the convergence of the calculated thermodynamic parameters with respect to the number of explicit solvent molecules. It has been shown that for the proton the hydration free energy is converged within ≈7 kJ/mol for $n = 5$ and 6 provided that the hydration energy is calculated as the interaction between the gas-phase proton and a hydrated water cluster, $H^+(g) + H_{2n}O_n(aq) \rightarrow H_{2n}O_{n+1}{}^+(aq)$. Here, we follow this approach and calculate the thermodynamics of hydration of OH from $OH(g) + H_{2n}O_n(aq) \rightarrow H_{2n+1}O_{n+1}(aq)$. We find that the hydration enthalpy is reasonably well converged within 10 kJ/mol. For the hydration free energy, the convergence is about 14 kJ/mol. We compute a hydration enthalpy of ≈−12 kJ/mol from MP2 calculations and ≈−17 kJ/mol from BHLYP. The hydration free energy is found to be positive ≈33 kJ/mol with MP2 and ≈15 kJ/mol with BHLYP.

The rest of the paper is organized as follows. Section II describes the computational and methodological procedures used

in our calculations. In section III, we present the structures of the $H_{2n+1}O_{n+1}$ clusters, the total energies, enthalpies, and free energies as well as the thermodynamic parameters of the hydration in the gas phase and in the aqueous phase. The results and their implications are discussed in section IV. Finally, the main conclusions are summarized in section V.

II. Method

Let E be the potential energy, (The potential energy is the sum of the electronic energy and the nuclear repulsion energy. Thus, U contains a kinetic energy term due to the movement of the electrons, which is included in the electronic energy term of the potential energy hypersurface defined by the nuclear positions according to the Born−Oppenheimer approximation.) U, enthalpy, H, or Gibbs free energy, G, of a closed shell $H_{2n}O_n$ or an open shell $H_{2n+1}O_{n+1}$ cluster. The hydration energy (U, H, or G) of OH in the gas phase for $H_{2n+1}O_{n+1}$ is

$$\Delta E_{gas}[OH,n] = E[H_{2n+1}O_{n+1}(g)] - (E[OH(g)] + E[H_{2n}O_n(g)]) \quad (1)$$

To obtain the quantities in eq 1, we begin by optimizing the geometries of $H_{2n}O_n$, $H_{2n+1}O_{n+1}$ clusters, and the free OH radical in the gas phase. This provides the quantities U[Y(g)], where, for simplicity, Y stands for $H_{2n}O_n$, $H_{2n+1}O_{n+1}$, or OH. Then, we calculate the harmonic frequencies for each optimized structure. This provides the vibrational enthalpy, including zero point vibrational energy, H_v(Y). The gas-phase enthalpies of species Y(g) is

$$H[Y(g)] = U(Y(g)) + H_R[Y(g)] + H_T[Y(g)] + H_V[Y(g)] + PV[Y(g)] \quad (2)$$

The rotational and traslational contributions are calculated from the ideal gas approximation ($H_R = H_T = 1.5RT$). The PV term is calculated from the molar volumes.

The gas-phase free energy is

$$G[Y(g)] = H[Y(g)] - TS[Y(g)] \quad (3)$$

where the gas-phase entropy, S[Y(g)], is calculated from the vibrational frequencies.

For the aqueous phase hydration, we calculate the thermodynamic parameters as

$$\Delta E_{hyd}[OH,n] = E[H_{2n+1}O_{n+1}(aq)] - (E[OH(g)] + E[H_{2n}O_n(aq)]) \quad (4)$$

The energy (U, H, and G) of species Y in the aqueous phase is calculated by including the solvent effects in the Hamiltonian of Y(aq) within self-consistent reaction field approximation (SCRF). Here, we make use of the PCM method.[44] Such a calculation yields the value of the SCRF hydration free energy, ΔG_{SCRF}(Y). Adding this quantity to the gas-phase free energy, we obtain the Gibbs free energy of species Y in the aqueous phase

$$G[Y(aq)] = G[Y(g)] + \Delta G_{SCRF}(Y) \quad (5)$$

Next we evaluate the entropy change due to the localized ordering of the solvent around species Y, ΔS_{SOLV}. This quantity is evaluated from the solvent accessible area following the method of Rashin and Namboodiri.[45] The SCRF hydration enthalpy and potential energy, ΔH_{SCRF} and ΔU_{SCRF}, which we will take as approximately equal, are calculated as

$$\Delta H_{SCRF} \equiv \Delta U_{SCRF} = \Delta G_{SCRF} + T\Delta S_{SOLV} \quad (6)$$

For H_9O_5 ($n = 4$) and $H_{11}O_6$ ($n = 5$), we have considered several structures. Hydration thermodynamics was calculated from averaged potential energies, enthalpies, and free energies. These were computed by performing a Boltzmann weighting over these geometries

$$E(Y) = \frac{\sum_{i=1}^{m_n} E_i(Y) e^{-\beta[G_i(Y)-G_1(Y)]}}{\sum_{i=1}^{m_n} e^{-\beta[G_i(Y)-G_1(Y)]}} \quad (7)$$

where m_n is the number of structures used in the average for $H_{2n+1}O_{n+1}$, Y stands for structure i of an gas-phase or aqueous-phase OH−water complex, β is the Boltzmann factor at room temperature, $RT = 2.5$ kJ/mol, and G_1[Y] is the free energy of most stable structure of species Y.

All of the quantum chemical calculations have been done with the Gaussian 98 program.[46] For each cluster size, we have made use of two different DFT approaches and the UMP2 method. The first DFT approach we have used consists of the Becke nonlocal exchange together with the Lee−Yang−Parr correlation potential (BLYP).[30] This method does not contain any exact, Hartree−Fock, exchange, and although it is computationally convenient, it will be shown to provide wrong results for OH−water interactions, at least for the smallest clusters with $n = 1-3$. The second DFT approach is the Becke's half and half (BH)[35] functional combined with the LYP corretalion (BHLYP). This hybrid functional combines 50% Becke's nonlocal exchange with 50% Hartree−Fock exchange.

The choice of the basis set for this work was a difficult one because we need to do geometry optimizations and frequency calculations at three different levels of theory for several structures of systems that contain up to 17 atoms. All these computations have to be done with a basis set that provides a suitable description of the interactions in the system. One of the main challenges was to avoid a large basis set superposition error (BSSE) for the calculation of a single hydrogen bond (HB), because several of these HB will have to be described for the larger clusters. Doing all of the geometry optimizations and frequency calculations with a good quality basis set such as 6-311++G(d,p)[47−50] that provides an accurate description of hydrogen bonding is beyond our current computational capabilities, especially for the larger clusters. Thus, we decided to optimize all of the geometries and calculate the vibrational frequencies with the cc-pVDZ[51] basis set. That basis set contains polarization functions on all atoms. It is known that such an attribute is important for an accurate description of this type of systems. Using this basis set requires about half of the computational resources for the SCF calculations and about one-third for the MP2 calculations as compared to the 6-311++G-(d,p). To obtain the values of U, H, and G, we start from U calculated with 6-311++G(d,p) at the geometry optimized with cc-pVDZ. Then, we take all of the vibrational contributions from the calculation with the cc-pVDZ basis set. This approximation will be accurate as long as the geometry and the vibrational frecuencies are not affected significantly by the choice of basis set, cc-pVDZ or 6-311++G(d,p). To test the accuracy of this mixed basis set (MBS) procedure for the description of hydrogen bonds, we studied the water dimer by means of the MBS and also by doing all of the optimizations and frequency calculations with the 6-311++G(d,p) basis set. The results are summarized

TABLE 1: Binding Energies of the Water Dimer in kJ/mol

	this work 6-311++G(d,p)			this work mixed cc-pVDZ/6-311++G(d,p)			BSSE corrected 6-31++G(d,p) (ref 52)		ref 53	ref 54
	BLYP	MP2	BHLYP	BLYP	MP2	BHLYP	MP2	B3LYP	CCSD(T)	expt
ΔU	−22.77	−25.43	−25.83	−11.55	−22.90	−24.79	−19.90	−21.61	−21.0 ± 0.2	
ΔH	−15.16	−17.83	−18.35	−3.37	−15.54	−17.40			−13.8 ± 0.4	−15.0 ± 2
ΔG	10.86	8.74	7.98	26.52	9.41	7.69				

TABLE 2: Energy, Enthalpy, and Free Energy of the OH Radical from the Mixed cc-pVDZ/6-311++G(d,p) Approach and from the Pure 6-311++G(d,p) Basis Set[a]

method	U_{gas}	H_{gas}	G_{gas}
BLYP	−75.7495/−75.7498	−75.7384/−75.7383	−75.7586/−75.7586
MP2	−75.5799/−75.5799	−75.5679/−75.5679	−75.5882/−75.5881
BHLYP	−75.7296/−75.7296	−75.7176/−75.7175	−75.7378/−75.7377

[a] All quantities in Hartree.

TABLE 3: Total Energies of the $H_{2n}O_n$ Clusters in Hartree as Calculated with the Mixed Basis Set Approach

method	n	U_{gas}	H_{gas}	G_{gas}	ΔE_{SCRF}	ΔG_{SCRF}	U_{aq}	H_{aq}	G_{aq}
BLYP	1	−76.4415	−76.4174	−76.4389	−30.83	−21.11	−76.4533	−76.4292	−76.4470
	2	−152.8874	−152.8362	−152.8678	−37.49	−21.48	−152.9017	−152.8505	−152.8760
	3	−229.3468	−229.2681	−229.3039	−46.81	−26.37	−229.3645	−229.2859	−229.3139
	4	−305.8077	−305.7026	−305.7458	−48.29	−23.20	−305.8261	−305.7210	−305.7547
	5	−382.2661	−382.1344	−382.1853	−58.83	−28.59	−382.2884	−382.1568	−382.1962
MP2	1	−76.2748	−76.2494	−76.2708	−35.10	−25.50	−76.2882	−76.2628	−76.2806
	2	−152.5584	−152.5047	−152.5381	−50.77	−34.49	−152.5777	−152.5240	−152.5512
	3	−228.8498	−228.7669	−228.8036	−51.77	−31.22	−228.8695	−228.7866	−228.8155
	4	−305.1448	−305.0335	−305.0775	−58.69	−33.40	−305.1671	−305.0558	−305.0902
	5	−381.4382	−381.2986	−381.3506	−68.98	−38.37	−381.4645	−381.3248	−381.3653
BHLYP	1	−76.41426	−76.3884	−76.4098	−32.71	−23.11	−76.4267	−76.4009	−76.4186
	2	−152.8380	−152.7835	−152.8168	−49.52	−33.31	−152.8568	−152.8024	−152.8294
	3	−229.2698	−229.1857	−229.2223	−47.63	−27.21	−229.2880	−229.2038	−229.2327
	4	−305.7042	−305.5914	−305.6354	−50.44	−25.33	−305.7234	−305.6106	−305.6450
	5	−382.1368	−381.9954	−382.0474	−63.27	−32.81	−382.1609	−382.0195	−382.0598

in Table 1, along with a comparison to other recent ab inito and experimental works.[52−54] These results show that the interaction energies, enthalpies, and free energies are significantly affected for the BLYP calculations only. For MP2 and BHLYP, the results from the MBS approach differ by ≈1 or 2 kJ/mol from those obtained by using the 6-311++G(d,p) basis set in the geometry and frequency calculations. The comparison between our results and those from rather high quality ab initio work as well as the experiment is encouraging. Thus, we proceed being aware that the inaccuracy of the MBS approach is not negligible for the BLYP calculations. In the next section, we present geometry optimizations and frequency calculations for H_3O_2 with the pure 6-311++G(d,p) basis set. These show that BLYP does not describe the OH−H_2O interaction correctly because of the overestimation of the self-interaction energy. However, MP2 and BHLYP calculations with both MBS approach and the pure 6-311+G(d,p) basis set provide further evidence that the mixed basis set method is accurate enough for the thermodynamics of the OH−water interaction.

III. Results

III.I. Water Clusters and Isolated OH. The total energies, enthalpies, and free energies for the OH radical for the three different methods as well as for the mixed basis set approach and the pure 6-311++G(d,p) basis set are reported in Table 2.

The structures of the $H_{2n}O_n$ ($n = 2-5$) clusters are rather similar to those presented previously in our work on H^+ and OH^- hydration.[42] Here, we started from these previous geometries and reoptimized them for the current level of theory. For $n = 3-5$, the clusters are cyclic structures in which each water acts as donor and acceptor in hydrogen bonds with the nearest neighbors. The total gas phase and aqueous phase energies, enthalpies, and free energies are summarized in Table 3. As a test of our computational procedure, we have calculated the hydration energy, enthalpy, and Gibbs free energy of water by using the equation

$$\Delta E_{hyd}[H_2O,n] = E[H_{2n+2}O_{n+1}(aq)] - (E[H_2O(g)] + E[H_{2n}O_n(aq)]) \quad (8)$$

TABLE 4: Thermodynamic Parameters in kJ/mol for Water Hydration Calculated as $H_2O(g) + H_{2n-2}O_{n-1}(aq) \rightarrow H_{2n}O_n(aq)$

method	n	ΔU_{hyd}	ΔH_{hyd}	ΔG_{hyd}
BLYP	1	−30.83	−30.83	−21.11
	2	−18.09	−10.14	26.05
	3	−56.06	−47.32	2.52
	4	−52.53	−46.15	−4.70
	5	−54.68	−48.31	−6.86
MP2	1	−35.10	−35.10	−25.50
	2	−38.74	−31.19	0.52
	3	−44.51	−34.60	17.06
	4	−59.87	−52.05	−10.24
	5	−59.08	−51.52	−10.98
BHLYP	1	−32.71	−32.71	−23.11
	2	−41.55	−34.25	−2.45
	3	−44.42	−33.97	17.25
	4	−55.50	−48.20	−6.56
	5	−61.09	−53.79	−13.07

The results are summarized in Table 4. There are two reported values of hydration enthalpy from experiment, −41.69 kJ/mol by Ben-Naim and Marcus[55] and −43.93 by Abraham et al.[56] Our calculations predict enthalpies that are more negative by several kJ/mol (by −7 to −13 kJ/mol). For the hydration free energy, we have found three different values in the literature. The oldest one is calculated from the difference in $\Delta G_f^0(H_2O)$

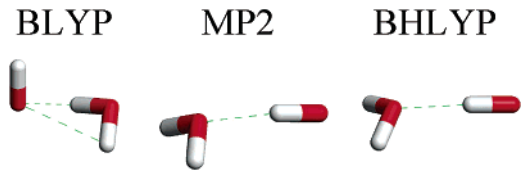

Figure 1. Optimized structures of H_3O_2.

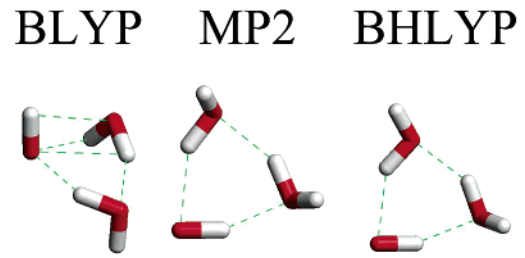

Figure 2. Optimized structures of H_5O_3.

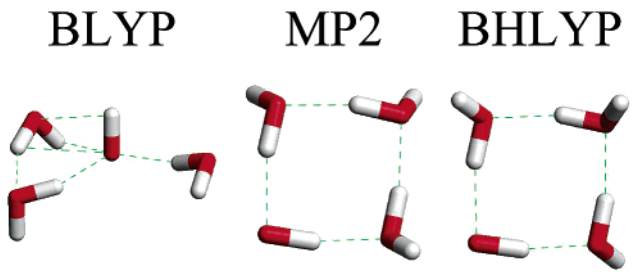

Figure 3. Optimized structures of H_7O_4.

between the gas and the liquid, −8.61 kJ/mol.[57] Ben-Naim and Marcus suggest that $\Delta G_{hyd}(H_2O) = -26.42$ kJ/mol.[55] Abraham et al.[56] report a hydration free energy of −8.57 kJ/mol. Our calculations point to value of hydration free energy of about −11 or −13 kJ/mol (MP2 and BHLYP respectively). These results are reasonably close to the values from experiment, although it is difficult to assess the reliability accurately because the experimental data span a range of ≈18 kJ/mol. To double check the MBS approach used here, we calculated the hydration free energy from a set of B3LYP/6-311++G(d,p) calculations by Tawa et al.,[40] who, fortunately, reported the total free energies of the water clusters. The calculated hydration free energies for $n = 1-6$ are, in kJ/mol, −25.47, −24.68, +16.01, −14.44, −8.66, and −4.46. They compare satisfactorily with our MP2/MBS and BHLYP/MBS results for $n = 1-5$.

III.II. $H_{2n+1}O_{n+1}$ Clusters. The structures of the $H_{2n+1}O_{n+1}$ clusters optimized with the cc-pVDZ basis set and the BLYP, MP2, and BHLYP methods are shown in Figures 1−5. Table 5 contains the results for H_3O_2 from both geometry optimization and vibrational frequencies with the 6-311++G(d,p). Table 6 summarizes the total energies, enthalpies, and free energies in the gas phase and in the aqueous phase for $n = 1-5$ as calculated with the mixed basis set approach. For H_9O_5 and $H_{11}O_6$ several energy minima have been studied (Figures 4 and 5). Their relative energies are reported in Table 7. The thermodynamic parameters (ΔU, ΔH, and ΔG) of complexation of OH with $H_{2n}O_n$ in the gas phase are summarized in Table 8.

For H_3O_2, we have considered the most stable structure only (Figure 1). For BLYP this consists of a hemibonded complex with a relatively short O−O distance of 2.3 Å. The optimization with the MP2 or BHLYP methods gives a rather different structure. We find that the most stable geometry is a hydrogen-bonded complex in which the radical acts as proton donor and water as proton acceptor, the O−O distance being ≈2.9 Å. This is actually the same type of structure that was reported by Wang et al.[22] for the ground state of H_3O_2. Geometry optimizations with the 6-311++G(d,p) basis set yield quite similar structures as with cc-pVDZ. The energies of complexation with the mixed basis set procedure and the pure 6-311++G(d,p) basis set are calculated from the data in Tables 2, 5, and 6. The results are

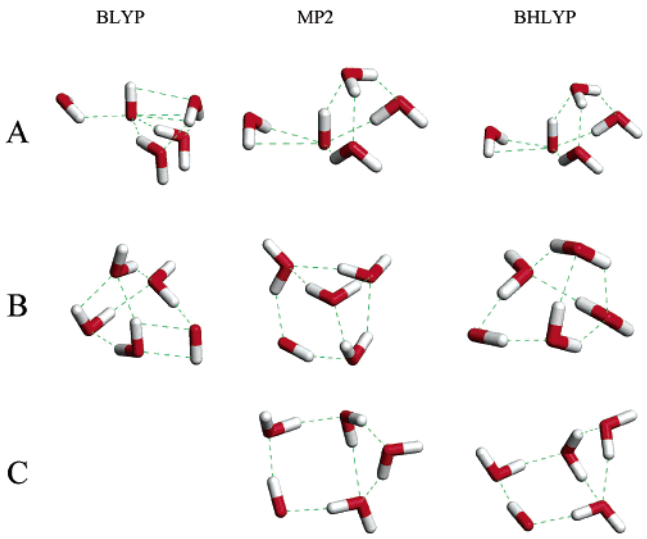

Figure 4. Optimized structures of H_9O_5.

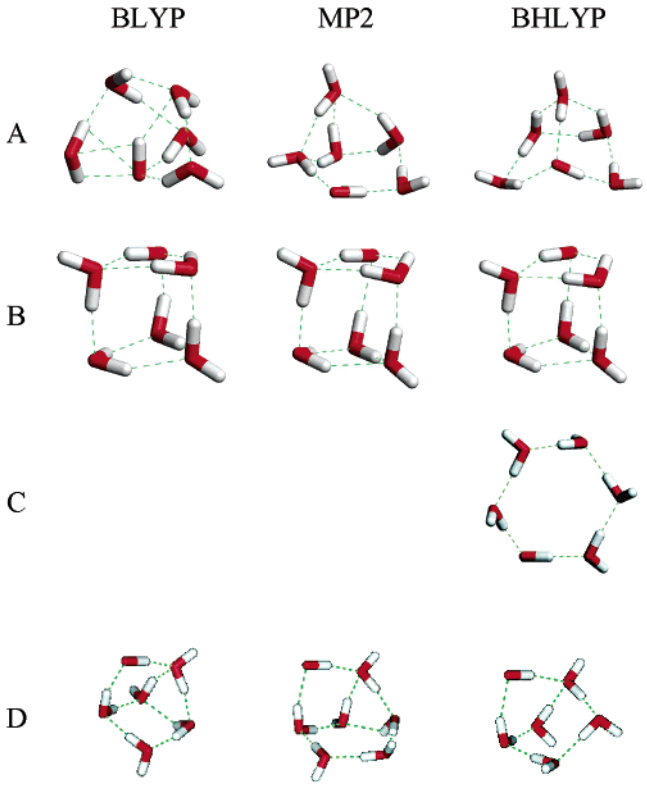

Figure 5. Optimized structures of $H_{11}O_6$.

TABLE 5: Total Potential Energy, Enthalpy, and Gibbs Free Energy of the H_2O-HO Complex and the Water Dimer Optimized with the 6-311++G(d,p) Basis Set[a]

	method	E_{gas}	H_{gas}	G_{gas}
H_3O_2	BLYP	−152.2048	−152.1666	−152.1981
	MP2	−151.8655	−151.8256	−151.8570
	BHLYP	−152.1555	−152.1151	−152.1474
H_2O	BLYP	−76.4418	−76.4174	−76.4389
	MP2	−76.2749	−76.2495	−76.2709
	BHLYP	−76.4144	−76.3885	−76.4100

[a] All quantitites are given in Hartree.

TABLE 6: Total Energies of the $H_{2n+1}O_{n+1}$ Clusters in the Gas Phase (U_{gas}, H_{gas}, and G_{gas}) and Aqueous Phase (U_{aq}, H_{aq}, and G_{aq}) in Hartee[a]

method	*n*	structure	U_{gas}	H_{gas}	G_{gas}	ΔU_{SCRF}	ΔG_{SCRF}	U_{aq}	H_{aq}	G_{aq}
BLYP	1		−152.2032	−152.16611	−152.1958	−37.69	−23.24	−152.2176	−152.1805	−152.2047
	2		−228.6600	−228.5948	−228.6301	−46.78	−27.59	−228.6778	−228.6126	−228.6406
	3		−305.1085	−305.0171	−305.0615	−54.77	−29.09	−305.1294	−305.0380	−305.0727
	4	A	−381.5605	−381.4420	−381.4932	−80.06	−49.49	−381.5910	−381.4724	−381.5120
		B	−381.5724	−381.4537	−381.5005	−56.14	−29.13	−381.5940	−381.4750	−381.5116
	5	A	−458.0160	−457.8695	−457.9225	−58.54	−26.54	−458.0383	−457.8918	−457.9325
		B	−458.0277	−457.8821	−457.9322	−40.89	−10.24	−458.0433	−457.8977	−457.9361
		D	−458.0255	−457.8801	−457.9326	−51.17	−19.10	−458.0450	−457.8996	−457.9400
MP2	1		−151.8646	−151.8248	−151.8562	−45.09	−29.55	−151.8818	−151.8419	−151.8674
	2		−228.1523	−228.0837	−228.1204	−44.16	−23.99	−228.1692	−228.1005	−228.1296
	3		−304.4446	−304.3477	−304.3925	−54.58	−29.59	−304.4654	−304.3685	−304.4038
	4	A	−380.7113	−380.5870	−380.6437	−73.52	−42.34	−380.7393	−380.6149	−380.6598
		B	−380.7326	−380.6066	−380.6565	−55.53	−27.55	−380.7537	−380.6277	−380.6669
		C	−380.7351	−380.6093	−380.6595	−60.30	−31.06	−380.7575	−380.6323	−380.6713
	5	A	−457.0285	−456.8742	−456.9301	−60.60	−27.38	−457.0515	−456.8973	−456.9405
		B	−457.0278	−456.8731	−456.9264	−48.11	−16.47	−457.0461	−456.8915	−456.9327
		D	−457.0297	−456.8754	−456.9316	−58.61	−25.37	−457.0520	−456.8977	−456.9413
BHLYP	1		−152.1550	−152.1147	−152.1460	−43.73	−28.30	−152.1717	−152.1314	−152.1568
	2		−228.5808	−228.5112	−228.5478	−41.21	−21.23	−228.5965	−228.5269	−228.5559
	3		−305.0181	−304.9197	−304.9633	−49.00	−24.20	−305.0368	−304.9384	−304.9725
	4	A	−381.4216	−381.2950	−381.3501	−66.92	−36.16	−381.4470	−381.3205	−381.3638
		B	−381.4352	−381.3076	−381.3563	−52.28	−24.33	−381.4551	−381.3275	−381.3655
		C	−381.4434	−381.3159	−381.3654	−52.68	−23.57	−381.4634	−381.3360	−381.3744
	5	A	−457.8620	−457.7082	−457.7607	−59.14	−26.50	−457.8620	−457.7307	−457.7708
		B	−457.8760	−457.7189	−457.7713	−46.70	−15.42	−457.8938	−457.7368	−457.7772
		C	−457.8784	−457.7229	−457.7837	−54.13	−21.48	−457.8991	−457.7435	−457.7919
		D	−457.8781	−457.7219	−457.778	−57.00	−23.95	−457.8998	−457.7436	−457.7871

[a] ΔU_{SCRF} and ΔG_{SCRF} are the hydration energies of the cluster as calculated with the PCM method, in kJ/mol.

TABLE 7: Relative Free Energies (kJ/mol) of the $H_{2n+1}O_{n+1}$ Clusters for Those Values of *n* for Which Several Structures Have Been Calculated

method	*n*	structure	ΔG_{gas}	ΔG_{aq}
BLYP	4	A	19.11	0
		B	0	1.08
	5	A	26.51	19.69
		B	1.13	10.24
		D	0	0
MP2	4	A	41.41	30.00
		B	7.77	11.38
		C	0	0
	5	A	3.93	1.99
		B	13.65	22.47
		D	0	0
BHLYP	4	A	40.24	27.70
		B	24.03	23.39
		C	0	0
	5	A	60.52	27.70
		B	32.62	23.39
		C	0	0
		D	14.96	12.60

TABLE 8: Thermodynamics of the Gas Phase Hydration of OH, $OH(g) + H_{2n}O_n(g) \rightarrow H_{2n+1}O_{n+1}(g)$[a]

method	*n*	ΔU	ΔH	ΔG
BLYP	1	−32.00 (−34.82)	−27.01 (−28.59)	4.58 (−1.78)
	2	−60.42	−53.15	−9.69
	3	−32.09	−28.10	2.62
	4	−40.77	−33.42	10.55
	5	−28.35	−21.27	30.72
MP2	1	−26.12 (−27.92)	−19.54 (−21.69)	7.28 (5.08)
	2	−37.07	−28.97	15.19
	3	−39.31	−33.69	−2.08
	4	−27.35	−20.54	16.61
	5	−29.93	−22.84	19.69
BHLYP	1	−29.43 (−30.21)	−22.80 (−24.11)	4.33 (0.39)
	2	−34.91	−26.68	17.68
	3	−49.03	−43.25	−8.27
	4	−25.19	−18.14	20.37
	5	−31.51	−25.99	3.93

[a] All of the quantities are given in kJ/mol. For those cluster sizes for which several structures were calculated, an average has been done (eq 7).

summarized in Table 8, in the entries for $n = 1$, where the energies from the optimization with the 6-311++G(d,p) basis set are shown in brackets. ΔU and ΔH differ by less than 2 kJ/mol in all cases. Free energies of complexation show a larger error, by about 6 kJ/mol for BLYP, 2 kJ/mol for MP2, and 4 kJ/mol for BHLYP. It is also noteworthy that the ΔU and ΔH values from BLYP are systematically more negative than those from MP2 or BHLYP. It is most likely that the hemibonded structure predicted by BLYP is not the true one but rather a consequence of the overestimation of the self-interaction energy in the exchange functional. This means that the BLYP approach, though computationally advantageous, is not suitable to study the hydration of OH. Moreover, adding some Hartree−Fock exchange seems to improve the DFT description of this interaction as compared to MP2. This is consistent with the results for the $H_4O_2^+$ complex by Sodupe et al.[34]

For H_5O_3 and H_7O_4, we find the same distinct behavior of BLYP with respect to MP2 and BHLYP (Figures 2 and 3). BLYP predicts the most likely structure to be a H_3O_2 hemibonded core plus one or two more waters that are directly bonded to the radical. In contrast, BHLYP and MP2 favor the formation of cyclic structures similar to those found for the closed shell water trimer and tetramer. These cyclic structures do not seem to be even energy minima for BLYP, because optimizations started from the MP2 geometries revert to the hemibonded structures. The energies, ΔU, and enthalpies, ΔH, of interaction of OH with H_4O_2 and H_6O_3 in the gas phase are predicted to be negative in all cases. Again, BLYP overestimates the strength of the interaction for $n = 2$. Interestingly, for clusters larger than H_5O_3, there is no clear overbinding of OH to $H_{2n-1}O_{n-1}$ calculated for BLYP as compared to MP2.

For the cluster H_9O_5 ($n = 4$), several structures have been studied (Figure 4). For BLYP, we begin from H_7O_4 and then

add one extra water that is hydrogen bonded to OH. This leads to the structure BLYP-A. We have also found a minimum by starting from the closed shell $H_{10}O_5$ ring from which a hydrogen atom has been removed so a H_2O is turned into an OH. After optimizing, the cyclic pentamer turns into the more compact BLYP-B structure in Figure 4. This second structure is the most stable one in the gas phase, the hemibonded complex being more stable in the aqueous phase. For MP2 and BHLYP, we have found three stable structures of H_9O_5. Structures MP2-A and BHLYP-A are obtained by starting geometry optimizations from BLYP-A. The hemibonded core of BLYP-A is turned into a water molecule with two hydrogen bonds to OH. Additionally, there are two rings containing the OH radical and two H_2O each. By starting from BLYP−B one gets the structures MP2−B and BHLYP−B, which can be described as four fused rings. Two of them contain waters and OH, and the other two include three waters. Finally, by starting from the cyclic water pentamer and removing a hydrogen atom, the MP2 and BHLYP optimizations lead to structures C, with a ring containing the OH and three waters and a ring with three waters. Structure C is the most stable one at both MP2 and BHLYP levels, followed by structrues B and A. The complexation energy, calculated by making use of eqs 7 and 1, show that the binding of OH to H_8O_4 is an exothermic process by about 20 kJ/mol. MP2 and BHLYP differ by ≈2 kJ/mol. The BLYP result is too exothermic by about 10 kJ/mol. The binding free energies are positive in all cases though.

For $H_{11}O_6$ ($n = 5$), we have started geometry optimizations from three different structures. We begin by describing the BLYP calculations first. An optimization started from the BLYP-A structure of the H_9O_5 cluster plus an additional water initially acting as a proton acceptor in a hydrogen bond to OH results in a structure in which the OH is surrounded by a cage-like water cluster. One of the waters seems to form a hemibond to OH, with a short O−O distance of 2.27 Å. We have also done optimizations that started from known stable structures of $H_{12}O_6$. The most stable water hexamer in aqueous phase is a cyclic one. By removing a hydrogen from this complex and optimizing at the BLYP level, one gets a trigonal prism geometry, with OH lying in a vertex. Another geometry optimization starting from the most stable gas-phase water hexamer, the trigonal prism, leads to the same structure BLYP-B, thus there is no BLYP-C structure because it is identical to BLYP-B. BLYP-B results to be more stable in both aqueous and gas phase than BLYP-A. For MP2 and BHLYP, starting from the BLYP-A complex leads to MP2-A and BHLYP-A structures in Figure 5. MP2-A contains two rings with the OH plus four waters and two rings containing three waters each. The BLYP-A type structure is not stable at the BHLYP level either. BHLYP-A consists of two cyclic tetramers sharing the OH and a ring containing three waters. The trigonal prism results to be a stable structure for both MP2 and BHLYP (structures MP2−B and BHLYP−B in Figure 5). Optimizations were also started from the water cyclic hexamer from which a H was removed. MP2 leads to the same trigonal prism, MP2-B, and BHLYP remains as a stable structure, BHLYP-C. We searched alternative energy minima by placing an OH inside a cyclic water pentamer. We find this to be an unfavorable situation. The optimized structures consist of an OH that is bonded in a donor−acceptor fashion to the water cluster (structures D in Figure 5). This structure is the most stable one for BLYP and MP2. For BHLYP, the structure C remains as the most stable one, although the energy difference with BLYP-D is small. In all cases, the attachment of OH to the $H_{10}O_5$ cluster in the gas phase is exothermic, with little to choose from BLYP or BHLYP as far as ΔU and ΔH is concerned. MP2 predicts a slightly less exothermic process by ≈3 kJ/mol. The binding Gibbs free energies are positive and more sensitive to the method than ΔU and ΔH.

The hydration energy, enthalpy, and Gibbs free energy has been calculated as the energy of the process $OH(g) + H_{2n}O_n(aq) \rightarrow H_{2n+1}O_{n+1}(aq)$ for $n = 1-5$. Averages have been taken according to eq 7 for $n = 4$ and 5. In all cases, the hydration enrgies, ΔU, and enthalpies, ΔH, are negative, such as was found for the gas-phase processes, the exothermicity is overestimated for BLYP with respect MP2 and BHLYP for $n = 1-2$. For $n \geq 3$ no clear trend is observed. We think that even if there was no overestimation of the interaction for $n \geq 3$ at the BLYP level, the calculated hydration ΔU and ΔH are less reliable than those from MP2 or BHLYP because of the disagreement found between the mixed basis set procedure and the optimizations with the 6-311++G(d,p) basis set. For MP2 and BHLYP the hydration energy tends toward ≈−20 kJ/mol and the enthalpy toward −17 or −22 kJ/mol. Although the MP2 results should be more reliable than the ones from BHLYP, the convergence of the energies with respect to cluster size seems to be worse for MP2 than for BHLYP. Thus, we cannot be sure which set of results is more accurate ($\Delta U = -19.42$ kJ/mol and $\Delta H = -12.86$ kJ/mol from MP2 or $\Delta U = -22.57$ kJ/mol or $\Delta H = -16.80$ kJ/mol from BHLYP). In any case, the hydration energy seems to converge to a value near −20 kJ/mol and the hydration enthalpy to somewhere near −15 kJ/mol.

The hydration free energies tend toward positive values for the three methods, although no clear trend is observed. For MP2, the difference between H_9O_5 and $H_{11}O_6$ is ≈15 kJ/mol. For BHLYP, the convergence is better, 7 kJ/mol from $n = 4$ to $n = 5$. However, there is a difference of 18 kJ/mol between the ΔG_{hyd} predicted by MP2 and BHLYP. The robustness of the MP2 and BHLYP methods found previously for the water dimer, for the hydration of water, and for the H_3O_2 complex suggests that the relatively wide range of values that are calculated here is caused by difficulties to find the most stable structures in the larger $OH-(H_2O)_n$ clusters.

IV. Discussion

Previous ab initio work by Wang et al.[22] shows that the MP2 method combined with a high quality basis set including diffuse and polarization functions provides reliable results for H_3O_2. Moreover, the mixed basis set approach used here, with energy optimizations and frequency calculations with the cc-pVDZ basis set and further single point calculation with 6-311++G(d,p) basis set, has been found to be reliable for the water dimer, hydration of water in the liquid, and the H_3O_2 complex. Thus, our MP2 calculations for $H_{2n+1}O_{n+1}$ ($n = 1-5$) could be regarded as a standard to which other simpler methods could be compared. The BLYP approach is not suitable for the description of the interaction between an OH radical and water as compared to MP2. The predicted structures are not correct, and the binding energy in the gas-phase is overestimated for small values of n. This is most likely caused by the lack of exact exchange in the functional such as shown by Sodupe et al. for $H_4O_2^+$ (ref 34). Curiously enough, by increasing the number of water molecules, the BLYP structures and energies begin to resemble those calculated by MP2. For example, both BLYP and MP2 predict that the most stable structure is a OH bonded as donor−acceptor to a water cyclic pentamer. The gas-phase binding energies, enthalpies, and free energies from

TABLE 9: Thermodynamics of Hydration of the OH Radical, $OH(g) + H_{2n}O_n(aq) \rightarrow H_{2n+1}O_{n+1}(aq)$[a]

method	n	ΔU	ΔH	ΔG
BLYP	1	−38.80	−34.00	2.42
	2	−69.94	−62.51	−15.85
	3	−40.19	−35.84	−0.21
	4	−43.59	−37.07	3.76
	5	−18.64	−11.55	38.86
MP2	1	−36.28	−29.55	3.35
	2	−30.45	−22.41	25.72
	3	−41.99	−36.57	−0.25
	4	−27.48	−22.32	18.72
	5	−19.42	−12.86	32.82
BHLYP	1	−40.34	−33.78	−0.90
	2	−26.57	−18.17	29.67
	3	−50.48	−44.70	−5.29
	4	−27.40	−20.48	22.02
	5	−22.57	−16.80	14.96

[a] All quantities are in kJ/mol. For those cluster sizes for which several structures were calculated, an average has been done (eq 7).

BLYP, −28.35, −21.27, and 30.72 kJ/mol, are not too different from those from MP2, $\Delta U_{gas} = -29.93$ kJ/mol, $\Delta H_{gas} = -22.84$ kJ/mol, and $\Delta G_{gas} = 19.69$ kJ/mol. BHLYP predicts structures and energies that are similar to those from MP2 for the cluster sizes studied here, although we always find differences of a few kJ/mol. The main difference between BHLYP and MP2 is found for $n = 5$. BHLYP predicts that the most stable structure of $H_{11}O_6$ is a ring of six molecules. In contrast MP2 predicts that the most likely structure of $H_{11}O_6$ is the OH hydrogen-bonded to a water pentamer, with the cyclic hexamer not even being a stable structure. Notwithstanding, $\Delta U_{gas}(H_{11}O_6)$ and $\Delta H_{gas}(H_{11}O_6)$ from BHLYP differ from those from MP2 by a few kJ/mol (≈5 kJ/mol) only. The difference between Gibbs free energies is larger, ≈15 kJ/mol.

The picture that arises from our results is that OH in water is involved in the formation of hydrogen bonds within cyclic structures resembling those for pure water. OH tends to form two or three hydrogen bonds, acting as proton donor and acceptor. Structures in which OH forms more than three hydrogen bonds, such as MP2-A for H_7O_4, are not favored energetically.

We have only found a previous set of theoretical results for the gas-phase hydration in water clusters $OH-H_{2n}O_n$ (n = 1−15). The reported ΔU_{gas} values from semiempirical PM3 for n = 1−5 are (in kJ/mol) −34.73, −32.32, −28.45, −27.59, and −21.71 (ref 16). These results are rather similar to our calculated ΔU_{gas} and ΔH_{gas}, so our work shows that these previous calculations were reasonably accurate, although no details on the structures were reported. We have found no previous thermodynamic data on the gas-phase complexation, $OH(g) + H_{2n}O_n(g) \rightarrow H_{2n+1}O_{n+1}(g)$ for $n > 1$ neither from experiment nor from accurate ab initio calculations. We report ΔU_{gas}, ΔH_{gas}, and ΔG_{gas} values that could be used as a reference for future experiments or calculations.

The binding energy of OH to gaseous clusters seems to converge with respect to cluster size to $\Delta U_{gas}(n \rightarrow \infty) = -30$ kJ/mol and $\Delta H_{gas}(n \rightarrow \infty) \approx -20$ or −25 kJ/mol. Coe et al.[16] extrapolated their PM3 results for the limit $n \rightarrow \infty$ and estimated a hydration energy of −35.70 kJ/mol. A more exact estimation of the hydration energy and enthalpy should be given by our set of results for $OH(g) + H_{2n}O_n(aq) \rightarrow H_{2n+1}O_{n+1}(aq)$ where the model for OH solvation includes both short-range specific effects and the long-range interaction with the polarizable continuum. The results from Table 9 point to $\Delta U_{hyd} \approx -20$ kJ/mol and $\Delta H_{hyd} \approx -12$ or −17 kJ/mol. These estimates of the hydration energy and enthalpy are ≈10 kJ/mol above those from the gas-phase clusters. The values of hydration potential energy, ΔU_{hyd}, of OH in the liquid are important for the determination of the adiabatic band gap of water. This band gap is the energy of the process

$$2H_2O(aq) \rightarrow OH(aq) + H_3O^+(aq) + e^-(cond) \qquad (9)$$

where e^-(cond) stands for an electron in the conduction band of the liquid. Because of the presence of OH(aq) on the right-hand side of this equation, the value of the band gap depends on ΔU_{hyd}(OH). Coe et al. used the value taken from the extrapolation of their PM3 calculations for gas-phase clusters,[16] $\Delta U_{hyd}(OH) = -35.70$ kJ/mol, and calculated a band gap of 6.89 eV. Our estimation of ΔU_{hyd}(OH) from the gas-phase clusters, −30 kJ/mol, leads to a band gap of 6.95 eV, which is rather close to the value by Coe et al.[16] However, by taking the hydration energy calculated from the hybrid solvation model, −20 kJ/mol, the estimated band gap is 7.05 eV; 0.16 eV larger than the previously reported value. In both cases, we estimate a band gap of water that is within the range of values reported in the literature,[58,59] 6.5−9.0 eV, and suggest a band gap close to 7 eV

For the hydration free energy, ΔG_{hyd}, the calculated values are positive by a few kJ/mol in all cases. It is difficult to extrapolate a value from the gas-phase clusters because the binding free energy, ΔG_{gas}, is converging slowly. For the aqueous-phase clusters, the convergence is slightly better but not as good as for ΔU_{hyd} and ΔH_{hyd}. If we consider the MP2 results only, the hydration energy should be somewhere near 20 or 30 kJ/mol. From BHLYP, one gets a lower energy of 15 or 20 kJ/mol. These results disagree by up to 40 kJ/mol with the values of standard hydration free energy reported previously in the literature. The measurement of the standard reduction potential of OH, E^0 (OH/OH^-), together with thermochemical data gives the value $\Delta G^0_{hyd}(OH) = -10.03$ kJ/mol (ref 21). Other calculations from standard free energy in thermochemical cycles suggest $\Delta G^0_{hyd}(OH) = -8.36$ kJ/mol (ref 60). These values are calculated for standard states consisting of a gas phase at $P = 1$ bar and a solution phase of unit molality. Our results refer to a different standard state in which the solution phase consists of a single OH in pure water (infinite dilution). We do not think that this should be responsible for the discrepancy between ΔG_{hyd}(OH) from calculation and from standard thermochemical data because the usual standard state for solution in molality scale is a hypothetical state with unity concentration and ideal behavior, as extrapolated from infinite dilution. The difference between our result, 15−30 kJ/mol, and those reported previously, −8 to −10 kJ/mol, is surprising provided the excellent results we got for $\Delta G_{hyd}(H_2O)$ and the test calculations for H_4O_2 and H_3O_2. It is more likely that this disagreement stems from the model used here, for example, use harmonic frequencies to calculate enthalpy and entropy or slow convergence with respect to cluster size rather than to the level of theory used. We would like to say that errors of up to 40 kJ/mol are usual in the determination of thermodynamic solvation data for ions by means hybrid solvent models and quantum mechanical calculations. Our problem here is that the solvation energy we try to calculate is in the same order of magnitude as the absolute error. In contrast, for ions, this same absolute error is a much smaller percentage of the total of hydration energy, typically a few hundreds of kJ/mol. We are currently improving our models by including different levels of theory, using larger water

clusters, and doing an exhaustive search of stable structures in the liquid phase.

V. Conclusions

We have presented a computational study of the hydration of OH in small aqueous clusters, $H_{2n+1}O_{n+1}$ ($n = 1-5$). We have employed three different quantum chemical methods to the study of these complexes.

First, we have done UMP2 calculations that, presumably, are reliable enough so as to take them as a reference.[22,34] The most stable structure of H_3O_2 is a hydrogen bonded complex with OH acting as a hydrogen donor. The calculated binding energies, $\Delta U \approx -27$ kJ/mol and $\Delta H \approx -20$ kJ/mol, agree well with the previously reported ones.[22] We also find an excellent agreement between our calculations for the water dimer and previous high quality ab initio and experimental results for H_4O_2. Calculations for the interaction of OH with the water dimer and trimer reveal that the most stable structures are rings similar to those found for H_6O_3 and H_8O_4. For larger complexes, H_9O_5 and $H_{11}O_6$, we find stable structures with the OH in cycles of 4 or 5 molecules. Formation of fused rings takes place when the strain associated with smaller cycles is balanced by the formation of new hydrogen bonds. Complexes in which OH acts a central unit surrounded by a solvation shell are less stable than the cyclic structures by up to 10 kJ/mol. The binding energies and enthalpies, $OH(g) + H_{2n}O_n(g) \rightarrow H_{2n+1}O_{n+1}(g)$ for $n > 1$, are negative by 20−30 kJ/mol. The most exothermic process is calculated for the formation of $H_5O_3(g)$. The free energies of complexation are positive by up to 20 kJ/mol or slightly negative, −2 kJ/mol for H_5O_3.

BLYP calculations predict wrong structures for most of the complexes as compared to the MP2 results. This is attributed to the lack of Hartree−Fock exchange in the Becke's exchange functional. Although that simplicity makes BLYP computationally faster, the self-exchange interaction is overestimated for the three-electron bond between a lone pair of H_2O and the unpaired electron of OH. The result is a hemibonded structure with a relatively short O−O (≈2.3 Å) distance for H_3O_2. For $H_5O_3-H_9O_5$, the BLYP structures consists of a hemibonded H_3O_2 core surrounded by a cage-like water cluster. The binding energies are overestimated as compared to MP2. Only for $n = 5$, $H_{11}O_6$, the BLYP structures resemble the stable MP2 geometries.

The problem of BLYP is solved, at least partially, by mixing 50% Hartree−Fock exchange to the Becke's functional (BHLYP). That brings the structures and the energies in much better agreement with MP2. That agreement is not perfect though. The ΔU, ΔH, and ΔG values from BHLYP differ by a few kJ/mol from those from MP2. The largest disagreement is found for $H_{11}O_6$, for which BHLYP predicts that the most stable structure is a quasi-planar cyclic hexamer in which all the molecules are forming two hydrogen bonds. In contrast, MP2 finds that the most stable complex is a compact structure in which OH form two hydrogen bonds, as a donor−acceptor.

We have also taken these gas-phase clusters as explicit models of the solvation shell of OH in liquid water. The long-range interactions with the solvent are added through a version of the self-consistent reaction field method,[36] here the PCM method,[44] to the Hamiltonian of the $H_{2n+1}O_{n+1}$ clusters. These calculations, combined with similar ones for the closed shell $H_{2n}O_n$ complexes, yield the quantities that are needed for the calculation of the energy, enthalpy, and Gibbs free energy of the process $OH(g) + H_{2n}O_n(aq) \rightarrow H_{2n+1}O_{n+1}(aq)$. These energies should converge to the hydration energy, enthalpy, and free energy of OH, ΔU_{hyd}, ΔH_{hyd}, and ΔG_{hyd}, in the limit of large values of n. Even for the small values of n considered here ($n = 1-5$), we find that the hydration energy and enthalpy are reasonably well converged within 10 kJ/mol. The calculated hydration energy $\Delta U_{hyd}(OH)$ seems to converge to a value near −20 kJ/mol. Previous estimations were based on semiempirical PM3 calculations for $n = 1-15$ and suggested $\Delta U_{hyd}(OH) \approx -36$ kJ/mol (ref 16). That value was found from an extrapolation for the gas-phase complexation, $OH(g) + H_{2n}O_n(g) \rightarrow H_{2n+1}O_{n+1}(g)$, for which we find $\Delta U \approx -30$ kJ/mol. Our hydration energy of −20 kJ/mol points to a value of the band gap of water near 7 eV. This supports the previous estimation by Coe et al.[16] We compute a hydration enthalpy of ≈−13 kJ/mol from MP2 calculations and ≈−17 kJ/mol from BHLYP.

The hydration free energy is found to be positive ≈32 kJ/mol with MP2 and ≈15 kJ/mol with BHLYP. These values are converged within ≈14 kJ/mol. Suggested values of $\Delta G^0_{hyd}(OH)$ found in the literature are −10 kJ/mol, from measurements of E^0 (OH/OH^-),[21] and −8.36 kJ/mol from thermochemical cycles and standard free energies of formation.[60] Our calculations for the hydration free energy of water, $H_2O(g) + H_{2n-2}O_{n-1}(aq) \rightarrow H_{2n}O_n(aq)$, point to $\Delta G_{hyd}(H_2O) = -11$ kJ/mol, MP2, and $\Delta G_{hyd}(H_2O) = -13$ kJ/mol, BHLYP. This is within the range of values reported in the literature, −8 to −26 kJ/mol. We also find a good agreement with $\Delta G_{hyd}(H_2O)$ from previous hybrid solvation models within the B3LYP/6-311++G(d,p) method.[40] The accuracy of our calculations is further supported by the comparisons for the water dimer and the $OH-H_2O$ complex to previous high quality ab initio data.[22] This suggests that the disagreement between the calculated and the previously reported $\Delta G_{hyd}(OH)$ values is most likely caused by the structures of the OH−water complexes here used. We have started energy optimizations from several structures based on previously studied water clusters. They seem to be suitable for the gas-phase, but we might be missing other structures with a lower free energy in the aqueous phase.

Acknowledgment. This work has been supported by DGES (PB98-0326) and the Plan Andaluz de Investigación (Grant FQ205). J.A.M. thanks Prof. Berend Smit for kindly granting access to the facilities of the Department of Chemical Engineering of the University of Amsterdam while writing this paper.

References and Notes

(1) Stumm, W.; Morgan, J. J. *Aquatic Chemistry*; Wiley: New York, 1996.
(2) Bielski, B. H. J.; Cabelli, D. E. Superoxide and Hydroxil radical Chemistry in Aqueous Solutions. In *Active Oxygen in Chemistry*; Foote, Ch. S., Valentine, J. S., Greenberg, A., Liebman, J. F., Eds.; Chapman& Hall: London, 1995; Vol. 2, pp 66−104.
(3) Spinks, J. W. T.; Woods, R. J. *An Introduction to Radiation Chemistry*, 3rd ed.; Wiley: New York, 1990
(4) Jay-Gerin, J.-P.; Ferradini, C. *Chem. Phys. Lett.* **2000**, *317*, 388.
(5) Chaychian, M.; Al-Sheikhly, M.; Silverman, J.; McLaughlin, W. L. *Rad. Phys. Chem.* **1998**, *53*, 145.
(6) Gårdfelt, K.; Sommar, J.; Strönberg, D.; Feng, X. *Atmos. Environ.* **2001**, *35*, 2001.
(7) Tripathi, G. N. R.; Sun, Q. *J. Phys. Chem. A* **1999**, *103*, 9055.
(8) Čik, G.; Šeršen, F.; Bumbálová, A. *Microporous Mesoporous Mater.* **2000**, *41*, 81.
(9) Chameides, W. L.; Davis, D. D. *J. Geophys. Res.* **1982**, *87*, 4863.
(10) Chameides, W. L. *J. Geophys. Res.* **1984**, *89*, 4739.
(11) Stemmler, K.; von Gunten, U. *Atmos. Environ.* **2000**, *34*, 4241.
(12) Ren, J.-G.; Xia, H.-L.; Just, T.; Dai, Y.-R. *FEBS Lett.* **2001**, *488*, 123.
(13) Linert, W.; Jameson, G. N. L. *J. Inorg. Biochem.* **2000**, *79*, 319.
(14) Cermenati, L.; Pichat, P.; Guillard, C.; Albini, A. *J. Phys. Chem. B* **1997**, *101*, 2650.
(15) Acero, J. L.; Stemmler, K.; von Gunten, U. *Environ. Sci. Technol.* **2000**, *34*, 591.

(16) Coe, J. V.; Earhart, A. D.; Cohen, M. H.; Hoffman, G. J.; Sarkas, H. W.; Bowen, K. H. *J. Chem. Phys.* **1997**, *107*, 6023.
(17) Hanson, D. R.; Burkholder, J. B.; Howard, C. J.; Ravishankara, A. R. *J. Phys. Chem.* **1992**, *96*, 4979.
(18) Takami, A.; Kato, S.; Shimono, A.; Koda, S. *Chem. Phys.* **1998**, *231*, 215.
(19) Staikova, M.; Donaldson, D. J. *Phys. Chem. Earth* **2001**, *26*, 473.
(20) Headrick, J. E.; Vaida, V. *Phys. Chem. Earth* **2001**, *26*, 479.
(21) Schwarz, H.; Dodson, R. W. *J. Phys. Chem.* **1984**, *88*, 3643.
(22) Wang, B.; Hou, H.; Gu, Y. *Chem. Phys. Lett.* **1999**, *303*, 96.
(23) Novakovskaya, Y. V.; Stepanov, N. F. *J. Phys. Chem. A* **1999**, *103*, 3285.
(24) Suh, M.; Bagus, P. S.; Pak, S.; Rosynek, M. P.; Lunsdorf, J. H. *J. Phys. Chem. B* **2000**, *104*, 2736.
(25) Ricca, A.; Bauschlicher, C. W., Jr. *Chem. Phys. Lett.* **2000**, *328*, 396.
(26) Wang, B.; Hou, H.; Gu, Y. *Chem. Phys. Lett.* **1999**, *309*, 274.
(27) Wang, L.; Hang, J. *J. Mol. Struct. (THEOCHEM)* **2001**, *543*, 167.
(28) Cremer, D.; Kraka, E.; Sosa, C. *Chem. Phys. Lett.* **2001**, *337*, 199.
(29) Parr, R. G.; Wang, W. *Density Functional Theory of Atoms and Molecules*; Oxford: New York, 1989.
(30) Becke, A. D. *J. Chem. Phys.* **1998**, *88*, 2547.
(31) Lee, C.; Yang, W.; Parr, R. G. *Phys. Rev. B* **1998**, *37*, 385.
(32) Noodleman, L.; Post, D.; Baerends, E. J. *Chem. Phys.* **1982**, *64*, 159.
(33) Bally, T.; Sastry, G. N. *J. Phys. Chem. A* **1997**, *101*, 7923.
(34) Sodupe, M.; Bertran, J.; Rodríguez-Santiago, L.; Baerends, E. J. *J. Phys. Chem. A* **1999**, *193*, 166.
(35) Becke, A. D. *J. Chem. Phys.* **1993**, *98*, 1372.
(36) Cramer, C. J.; Thrular, D. G. *Chem. Rev.* **1999**, *99*, 2161.
(37) Sánchez Marcos, E.; Pappalardo, R. R.; Rinaldi, D. *J. Phys. Chem.* **1991**, *95*, 8928.
(38) Martínez, J. M.; Pappalardo, R. R.; Sánchez Marcos, E. *J. Phys. Chem. A* **1997**, *101*, 4444.
(39) Tuñón, I.; Silla, E.; Bertrán, J. *J. Phys. Chem.* **1993**, *97*, 5547.
(40) Tawa, G. J.; Topol, I. A.; Kurt, S. K.; Caldwell, R. A.; Rashin, A. A. *J. Chem. Phys.* **1998**, *109*, 4852.
(41) Topol, I. A.; Tawa, G. J.; Burt, S. K.; Rashin, A. A. *J. Chem. Phys.* **1999**, *111*, 10998.
(42) Mejías, J. A.; Lago, S. *J. Chem. Phys.* **2000**, *113*, 7306.
(43) Mejías, J. A.; Hamad, S.; Lago, S. *J. Phys. Chem. A* **2002**, *106*, in press.
(44) V. Barone, M. Cossi and J. Tomasi *J. Comput. Chem.* **1998**, *19*, 404.
(45) Rashin, A. A.; Namboodiri, K. *J. Phys. Chem.* **1987**, *91*, 6003.
(46) Frisch, M. J.; Trucks, G. W.; Schlegel, H. B.; Scuseria, G. E.; Robb, M. A.; Cheeseman, J. R.; Zakrzewski, V. G.; Montgomery, J. A., Jr.; Stratmann, R. E.; Burant, J. C.; Dapprich, S.; Millam, J. M.; Daniels, A. D.; Kudin, K. N.; Strain, M. C.; Farkas, O.; Tomasi, J.; Barone, V.; Cossi, M.; Cammi, R.; Mennucci, B.; Pomelli, C.; Adamo, C.; Clifford, S.; Ochterski, J.; Petersson, G. A.; Ayala, P. Y.; Cui, Q.; Morokuma, K.; Malick, D. K.; Rabuck, A. D.; Raghavachari, K.; Foresman, J. B.; Cioslowski, J.; Ortiz, J. V.; Stefanov, B. B.; Liu, G.; Liashenko, A.; Piskorz, P.; Komaromi, I.; Gomperts, R.; Martin, R. L.; Fox, D. J.; Keith, T.; Al-Laham, M. A.; Peng, C. Y.; Nanayakkara, A.; Gonzalez, C.; Challacombe, M.; Gill, P. M. W.; Johnson, B. G.; Chen, W.; Wong, M. W.; Andres, J. L.; Head-Gordon, M.; Replogle, E. S.; Pople, J. A. *Gaussian 98*; Gaussian, Inc.: Pittsburgh, PA, 1998.
(47) McLean, A. D.; Chandler, G. S. *J. Chem. Phys.* **1980**, *72*, 5639.
(48) Krishnan, R.; Binkley, J. S.; Seeger, R.; Pople, J. A. *J. Chem. Phys.* **1980**, *72*, 650.
(49) Clark, T.; Chandrasekhar, J.; Spitznagel, G. W.; Schleyer, P. v. R. *J. Comput. Chem.* **1983**, *4*, 294.
(50) Frisch, M. J.; Pople, J. A.; Binkley, J. S. *J. Chem. Phys.* **1984**, *80*, 3265−3269.
(51) Woon, D. E.; Dunning, T. H., Jr. *J. Chem. Phys.* **1993**, *98*, 1358.
(52) Simon, S.; Bertran, J.; Sodupe, M. *J. Phys. Chem. A* **2001**, *105*, 4359.
(53) Klopper, W.; van Duijneveldt−van de Rijdt, J. G. C. M.; van Duijnevelt, F. B. *Phys. Chem. Chem. Phys.* **2000**, *2*, 2227.
(54) Curtiss, L. A.; Frurip, D. J.; Blander, M. *J. Chem. Phys.* **1979**, *71*, 2703.
(55) Ben-Naim, A.; Marcus, Y. J. *Chem. Phys.* **1984**, *81*, 2016.
(56) Abraham, M. H.; Whiting, G. S.; Fuchs, R.; Chambers, E. J. *J. Chem. Soc., Perkin Trans. 2* **1990**, 291.
(57) Wagman, D. D.; Evans, W. H.; Parker, V. B.; Schumm, R. H.; Halow, I.; Bailey, S. M.; Churney, K. L.; Nuttall, R. L. The NBS tables of chemical thermodynamic properties. Selected values for inorganic and C1 and C2 organic substances in SI units. *J. Phys. Chem. Ref. Data* **1982**, *11*, Suppl No. 2.
(58) Grand, D.; Bernas, A.; Amouyal, E. *Chem. Phys.* **1979**, *44*, 73.
(59) Han, P.; Bartels, D. M. *J. Phys. Chem.* **1990**, *94*, 5824.
(60) Golden, D. M.; Bierbaum, V. M.; Howard, C. J. *J. Phys. Chem.* **1990**, *94*, 5413.